


## ARTICLE OPEN

## Mathematical model of hemodynamic mechanisms and consequences of glomerular hypertension in diabetic mice

Hari Shankar Mahato<sup>1</sup> , Christine Ahlstrom<sup>2</sup>, Rasmus Jansson-Löfmark<sup>2</sup>, Ulrika Johansson<sup>3</sup>, Gabriel Helmlinger<sup>4</sup> and K. Melissa Hallow<sup>1</sup>

Many preclinically promising therapies for diabetic kidney disease fail to provide efficacy in humans, reflecting limited quantitative translational understanding between rodent models and human disease. To quantitatively bridge interspecies differences, we adapted a mathematical model of renal function from human to mice, and incorporated adaptive and pathological mechanisms of diabetes and nephrectomy to describe experimentally observed changes in glomerular filtration rate (*GFR*) and proteinuria in db/db and db/db UNX (uninephrectomy) mouse models. Changing a small number of parameters, the model reproduced interspecies differences in renal function. Accounting for glucose and Na<sup>+</sup> reabsorption through sodium glucose cotransporter 2 (SGLT2), increasing blood glucose and Na<sup>+</sup> intake from normal to db/db levels mathematically reproduced glomerular hyperfiltration observed experimentally in db/db mice. This resulted from increased proximal tubule sodium reabsorption, which elevated glomerular capillary hydrostatic pressure ( $P_{gc}$ ) in order to restore sodium balance through increased GFR. Incorporating adaptive and injurious effects of elevated  $P_{gc}$ , we showed that preglomerular arteriole hypertrophy allowed more direct transmission of pressure to the glomerulus with a smaller mean arterial pressure rise; Glomerular hypertrophy allowed a higher GFR for a given  $P_{gc}$ ; and  $P_{gc}$ -driven glomerulosclerosis and nephron loss reduced GFR over time, while further increasing  $P_{gc}$  and causing moderate proteinuria, in agreement with experimental data. UNX imposed on diabetes increased  $P_{gc}$  further, causing faster GFR decline and extensive proteinuria, also in agreement with experimental data. The model provides a mechanistic explanation for hyperfiltration and proteinuria progression that will facilitate translation of efficacy for novel therapies from mouse models to human.

npj Systems Biology and Applications (2018)4:41; <https://doi.org/10.1038/s41540-018-0077-9>

## INTRODUCTION

Diabetic kidney disease is a growing health problem worldwide, yet the development of novel therapeutic treatments remain challenging. There have been multiple experimental therapies with promising efficacy attributes in preclinical studies, which have not yielded efficacy in humans.<sup>1</sup> Part of the challenge is that we do not fully understand quantitative and kinetic aspects of how kidney disease in rodent models of diabetic nephropathy develops, progresses, and differs from humans. Such gaps in our understanding can result in a flawed interpretation of preclinical efficacy data of novel experimental compounds. Mathematical modeling can be a useful tool in quantitatively bridging differences in disease processes, time courses of progression, and responses to therapies across species.<sup>2</sup>

In humans, early diabetic kidney disease is characterized by glomerular hyperfiltration, hypertrophy of the glomerulus and tubules, and development of microalbuminuria. This early injury is followed by progressive glomerulosclerosis, overt proteinuria, nephron loss, and ultimately renal failure.<sup>3,4</sup> Advanced diabetic nephropathy developing over decades in humans is difficult to address in animal models. Only a few of the available diabetic nephropathy rodent models exhibit most of the characteristics of human diabetic nephropathy, secondary to Type 2 diabetes

mellitus. Mouse models with deficient leptin production (black and tan, brachyuric (BTBR) ob/ob mouse) or dysfunctional leptin signaling (db/db mouse) have shown promising results in mimicking human disease progression.<sup>5,6</sup> The BTBR ob/ob mouse model develops glomerular lesions with progressive proteinuria at a young age; however, a major concern with these mice is their infertility, resulting in difficulties in breeding.<sup>6</sup> The db/db mouse model demonstrates characteristics of early human diabetic kidney disease, such as hypertrophy, hyperfiltration, and albuminuria,<sup>7</sup> and appears to most closely mimic the progression of mesangial matrix expansion seen in humans.<sup>7</sup> However, disease progression in the db/db model, including mesangial matrix expansion, is slower than in the BTBR ob/ob and only mild proteinuria may develop.<sup>7,8</sup> Uninephrectomy (UNX) at 6–8 weeks of age in db/db mice has proven to accelerate the development of late stage diabetic nephropathy, with mice exhibiting mesangial matrix expansion and overt albuminuria at an age of 20–22 weeks consistent with abnormalities of advanced human diabetic kidney disease.<sup>3</sup> The db/db UNX mouse model is commonly used in preclinical drug development programs, to evaluate drug targets and compounds and to inform efficacy predictions in a human diabetic nephropathy population. Even though this animal model exhibits a majority of characteristics seen in the human

<sup>1</sup>School of Chemical, Materials, and Biomedical Engineering, University of Georgia, Athens, GA, USA; <sup>2</sup>Drug Metabolism and Pharmacokinetics, Cardiovascular, Renal, and Metabolism, Innovative Medicines and Early Development Biotech Unit, AstraZeneca, Gothenburg, Sweden; <sup>3</sup>Bioscience Chronic Kidney Disease, Cardiovascular, Renal, and Metabolism Innovative Medicines and Early Development Biotech Unit, AstraZeneca, Gothenburg, Sweden and <sup>4</sup>Quantitative Clinical Pharmacology, Innovative Medicines and Early Development Biotech Unit, AstraZeneca, Waltham, MA, USA

Correspondence: K Melissa Hallow (hallowkm@uga.edu)

Received: 14 September 2017 Revised: 29 June 2018 Accepted: 22 October 2018

Published online: 10 December 2018

population, translation of efficacy and of its time course to patients remains challenging. A quantitative mathematical disease model that incorporates common processes of renal injury, as well as between-species differences, may improve our ability to interpret data within this translation process.

We previously described a mathematical model of renal function and sodium ( $\text{Na}^+$ ) and volume homeostasis.<sup>9</sup> This model was developed with data from human and rat studies. We used the model to demonstrate the tubular hypothesis of diabetic hyperfiltration,<sup>10</sup> whereby hyperfiltration in early diabetes is an indirect consequence of increased proximal tubule (PT)  $\text{Na}^+$  reabsorption. We further showed that increased PT  $\text{Na}^+$  reabsorption in diabetes contributes to increased glomerular hydrostatic pressure (especially when regulation of tubular  $\text{Na}^+$  handling is impaired) and proposed that this may represent an initiating step in diabetic kidney disease progression.<sup>11</sup>

In the present modeling study, we first show that the same mathematical model of normal renal physiology may be reparameterized to reproduce renal function in mice, rats, and humans. We then extend this model to represent adaptive and pathological changes that occur following development of diabetes and nephrectomy, focusing on the db/db and db/db UNX mouse models of kidney disease.

## RESULTS

### Translating normal renal function across species

The core model of renal function, illustrated in Fig. 1, was originally developed to describe normal human physiology.<sup>9,11</sup> We first aimed to reparametrize this model to represent normal rat and mouse renal function. The key underlying processes of renal blood flow, filtration, reabsorption, excretion, and systemic volume homeostasis were assumed to be structurally the same across different species. Thus, model equations remained unchanged across species; only model parameter values were changed. These parameter values, along with measurable model variables (e.g., *glomerular filtration rate [GFR]*, *mean arterial pressure [MAP]*, *cardiac output [CO]*) were determined, for each species, from literature sources. Resistance parameters were calculated based on other parameters and variables, as described previously.<sup>9</sup> For instance, rather than specifying total peripheral resistance, it was instead calculated for each species based on that species' normal mean arterial pressure and cardiac output.

Model parameter values for each species, given in Table 1, were used to reproduce the phenotypic behavior for each species, as listed in Table 2. Many morphologic and functional parameters are conserved across species. Arteriole and tubular diameters, the ultrafiltration coefficient, and plasma concentrations of glucose and  $\text{Na}^+$  are highly consistent across species. Other parameters vary widely across species, in accordance with body weight. The number of nephrons ( $N_{\text{nephrons}}$ ), the extracellular fluid volume (ECF),  $\text{Na}^+$  ( $N_{\text{a, in}}$ ), water ( $W_{\text{in}}$ ), and food ( $F_{\text{in}}$ ) intakes all vary by orders of magnitude, presumably partly influenced by species size.

Pressures (e.g., MAP, glomerular hydrostatic pressure, tubular pressures, etc.) are also quite similar across species, while flow rates (CO, RBF, GFR) vary by orders of magnitude. Interestingly, while GFR varies widely across species, single nephron GFR is highly conserved. In larger species, a higher GFR is achieved through an increased number of nephrons, while single-nephron flow and pressure metrics are remarkably similar.

### Composite profile of disease progression in db/db and db/db UNX mice

We next sought to use the model to mechanistically and quantitatively describe the pathophysiological processes that produce disease progression observed in obese leptin receptor deficient db/db mice. There is considerable variability in the levels

of blood glucose, proteinuria, and GFR reported among studies in db/db mice. Thus, rather than relying on a single study to inform the model, a composite dataset was developed from all identified published studies for which either urinary albumin excretion rate, GFR, or both were reported in db/db mice, with or without UNX. In addition, data from three unpublished AstraZeneca studies, conducted according to the protocols of Huang 2008,<sup>12</sup> were included. These data are summarized in Fig. 2. In all studies in which UNX mice were included, uninephrectomy was conducted between weeks 8 and 10. Blood glucose was stable in WT and db/m mice, but increased over time in db/db mice (both UNX and non-UNX) to reach levels between 400 and 600 mg/dl in most studies. GFR was elevated in db/db mice compared to wild type and db/m, as expected. Although few studies in db/db UNX mice reported GFR, one study<sup>13</sup> found GFR higher than WT and db/m but lower than db/db non-UNX at week 15, and another study<sup>12</sup> found GFR similar to WT and falling from week 20–22. These data suggest that GFR recovers after UNX to near levels of non-UNX, but then declines more rapidly over time compared to db/db non-UNX mice. The urinary albumin excretion rate (UAER) increased over time in db/db mice, and increased more rapidly in db/db UNX mice following uninephrectomy.

### Modeling hyperfiltration in the db/db mouse model

To mathematically reproduce functional renal changes observed in db/db non-UNX mice, blood glucose was allowed to increase over time, in the model, up to 500 mg/dl, consistent with data shown in Fig. 2. Sodium and water were increased by 1.5 and 5.0-fold, respectively, consistent with reported levels from studies described above. Data from these studies also point to minimal urinary glucose excretion (UGE) in animals with plasma glucose concentrations of less than 400 mg/dl (note: this is a much higher capacity than is typically observed in humans, where glucose excretion occurs for plasma levels above ~250 mg/dl).<sup>14,15</sup> This suggests that, as animals become diabetic, the PT capacity for glucose reabsorption increases sufficiently, so that all filtered glucose is still reabsorbed, at least up to 400 mg/dl. Thus, the renal threshold for glucose reabsorption, RTg, was increased to 400 mg/dl. Simulations were first conducted without considering any additional adaptive or maladaptive changes.

As shown in Fig. 3 (dark blue color), as glucose increased over time, GFR also increased, although the increase slowed down once glucose reached the RTg threshold value of 400 mg/dl. The reason for this phenomenon is as follows: increased plasma glucose results in more glucose being filtered through the glomerulus. For glucose levels below the threshold RTg value of 400 mg/dl,<sup>14,15</sup> all the excess glucose is reabsorbed in the PT. Since  $\text{Na}^+$  and glucose reabsorption processes are coupled through the SGLT2 transporter, PT fractional  $\text{Na}^+$  reabsorption is increased as well (Fig. 3c), producing a sodium imbalance. The only ways to restore  $\text{Na}^+$  balance are to: a) reabsorb less  $\text{Na}^+$ ; or b) filter more  $\text{Na}^+$ . While the model accounts for some compensation through changes in tubular  $\text{Na}^+$  reabsorption, these adaptations are not sufficient.<sup>11</sup> Thus, over time,  $\text{Na}^+$  and water were retained (Fig. 3d), driving up mean arterial pressure and glomerular pressure (Fig. 3e, f), thus increasing GFR up until sodium balance is returned. We previously described this mechanism for diabetic hyperfiltration in detail.<sup>11</sup>

### Kidney adaptation and injury in response to diabetes and glomerular hypertension

The simulations described above showed that diabetes can produce an increase in GFR and glomerular hypertension, but did not yet account for adaptive and maladaptive changes accompanying these effects. These simulations predicted a large increase in MAP (40 mmHg), as well as an associated increase in preglomerular vascular resistance, as myogenic autoregulation attempts to prevent transmission of increased systemic pressure

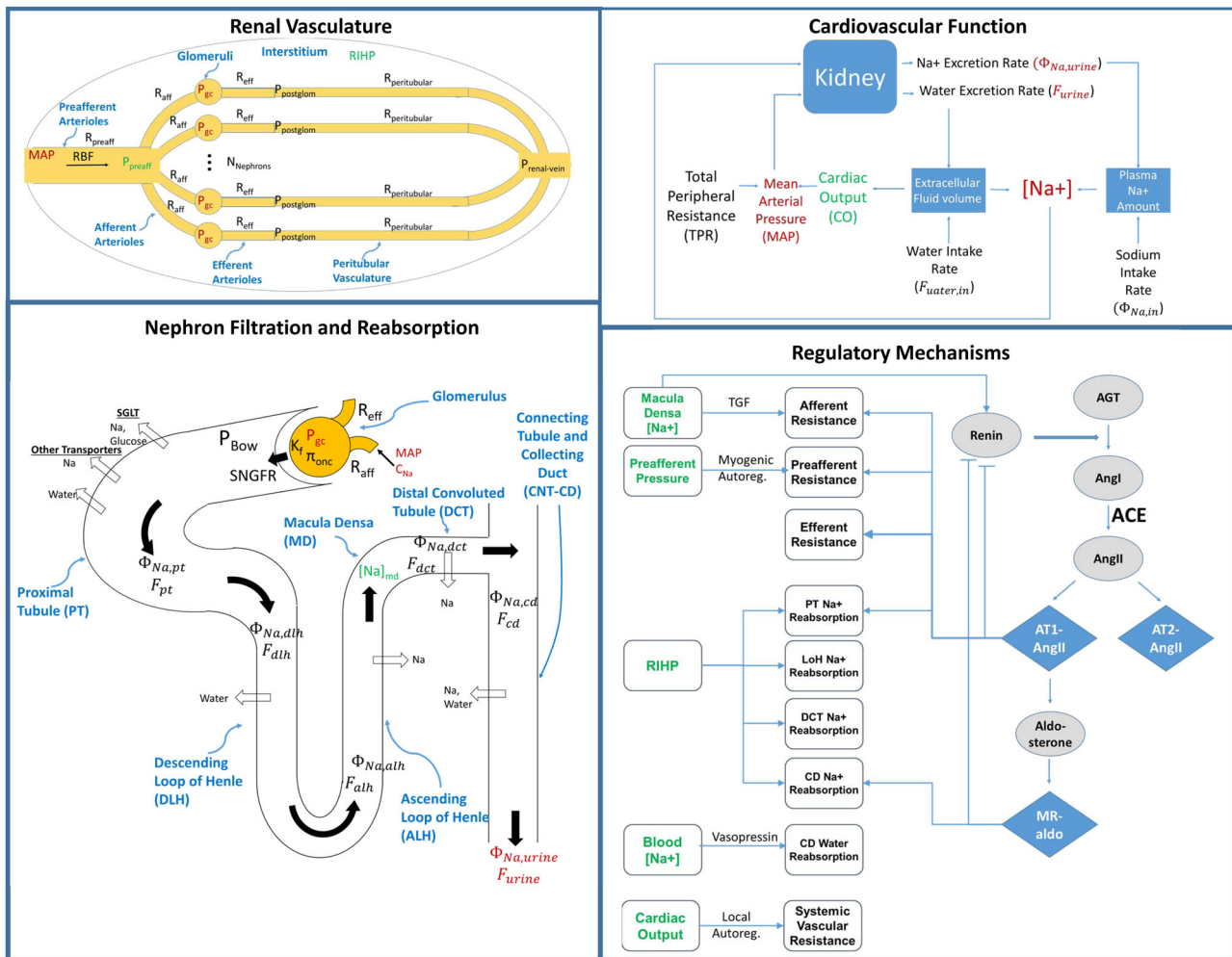


**Fig. 1** Schematic representation of the base model of renal CNT function. (Top Left) The renal vasculature is modeled by a single preafferent resistance vessel flowing into  $N$  parallel nephrons. Bottom Left)  $\text{Na}^+$  and water filtration through the glomerulus are modeled according to Starling's law.  $\text{Na}^+$  and water are reabsorbed at different fractional rates in the proximal tubule, loop of Henle, distal convoluted tubule, and connecting tubule/collecting duct, and  $\text{Na}^+$  and water excretion rates are determined from unabsorbed  $\text{Na}^+$  and water. Top right)  $\text{Na}^+$  and water excretion feed into the cardiovascular portion of the model, where the balance between excretion and intake determines extracellular fluid volume, plasma  $\text{Na}^+$  concentration, cardiac output (CO) and ultimately mean arterial pressure (MAP).  $\text{Na}^+$  concentration and MAP feed back into the renal model (left), closing the loop. Bottom Right) Multiple regulatory mechanisms, including the renin-angiotensin-aldosterone system (RAAS), tubulo-glomerular feedback (TGF), myogenic autoregulation, renal interstitial hydrostatic pressure (RIHP) regulation of tubular  $\text{Na}^+$  reabsorption, vasopressin regulation of tubular water reabsorption, and local blood flow autoregulation, provide feedbacks on model variables, to maintain or return homeostasis

to the glomerulus—but db/db mice do not consistently develop hypertension. Afferent arteriole diameters have been found to be 25% larger in db/db mice compared to db/m.<sup>16</sup> The same study found that myogenic autoregulation in db/db mice was intact, although studies in other models of diabetes have shown autoregulatory impairment.<sup>17</sup> Increased afferent diameter may allow MAP to be more directly transmitted to the glomerulus. In addition, in both humans and animal models of diabetes, the early diabetic kidney is characterized by glomerular and tubular hypertrophy.<sup>18,19</sup> Similar patterns of hypertrophy are observed in the remaining kidney following nephrectomy in both mice and humans.<sup>13,20</sup> This hypertrophy response is likely an adaptation to accommodate increased demands for filtration and reabsorption. Across species, this process occurs quickly (over weeks to months), and glomerular volume increases as much as 50%.<sup>13,21,22</sup> As diabetic kidney disease progresses, glomerulosclerosis, the scarring or thickening of the glomerular basement membrane, occurs, and podocytes become damaged, all leading to proteinuria. Excess protein in the tubules accelerates the rate of disease

progression, likely by stimulating inflammation, resulting in tubular injury, fibrosis, and ultimately nephron loss.<sup>23</sup> Although multiple factors may be involved, elevated glomerular hydrostatic pressure is believed to be a major driver of these processes.<sup>24</sup> We have incorporated these adaptive and pathological consequences of elevated glomerular hydrostatic pressure into the model, through changes over time in model parameters, as illustrated in Fig. 4.

#### Afferent Arteriole dilatation

When afferent arterioles were allowed to increase in diameter up to 25% in response to elevated blood glucose, the model showed that the same rise in  $GFR$  was achieved with a much smaller increase in MAP compared to the case without afferent dilatation (Fig. 3, medium blue line). Because preglomerular resistance did not rise, increases in MAP were more directly transmitted to the glomerulus, allowing  $GFR$  to increase and sodium balance to be restored at a much lower systemic pressure.

**Table 1.** Model parameters for human, rat, and mouse

Parameter	Symbol	Units	Human	Rat	Mouse
Parameters that differ by species					
Number of nephrons	$N_{\text{nephrons}}$	–	$2 \times 10^6$	50,000	10,000
Sodium intake	$Na_{\text{in}}$	mmol/day	100	2	0.576
Water intake	$Wa_{\text{in}}$	L/day	2	0.025	0.005
Proximal tubule length	$L_{\text{pt}}$	mm	14	5	2.2
Plasma protein concentration	$C_p$	g/dl	7	6.2	3.4
Parameters conserved across species					
Plasma glucose level		mg/dl	90	90	90
Plasma sodium concentration	$C_{\text{Na}}$	mmol/L	140	140	140
Glomerular ultrafiltration coefficient	$K_{f,0}$	nl/min-mmHg	3.9	3.9	3.9
Albumin sieving coefficient	$K_{\text{albumin}}$	–	0.0006	0.0006	0.0006
Renal capacity for albumin reabsorption	$RC_{\text{albumin}}$	mg/min	$2.5 \times 10^{-6}$	$2.5 \times 10^{-6}$	$2.5 \times 10^{-6}$
Efferent arteriole diameter	$D_{\text{eff}}$	$\mu\text{m}$	11	10.5	10.5
Afferent arteriole diameter	$D_{\text{aff}}$	$\mu\text{m}$	14.5	14	14
Proximal tubule diameter	$D_{\text{pt}}$	$\mu\text{m}$	27	27	27
Renal threshold for glucose reabsorption	$RT_g$	mg/dl	180	180	180
Fractional PT Na reabsorption		$\eta_{\text{pt,non-SGLT2}}$	0.76	0.76	0.76
Calculated parameters					
Renal vascular resistances	$R_{\text{rvr}}$	mmHg-L/min	81	8727	58,180
Peritubular resistance	$R_{\text{peri}}$	mmHg-L/min	5.766	537	2700
Preafferent resistance	$R_{\text{prea}}$	mmHg-L/min	14	3500	23,000
Total peripheral resistance	$R_{\text{rpr}}$	mmHg-L/min	18.6	258	1114
Parameters of kidney adaptation and injury					
Maximum afferent arteriole diameter increase	$\Delta D_{a,\text{max}}$				25%
Maximum increase in surface area	$\Delta SA_{\text{max}}$				50%
Maximum increase in permeability	$\Delta \text{Perm}_{\text{max}}$				100%
Time constant for increase in afferent diameter	$\tau_{\text{daa}}$				$4 \times 10^6$
Time constant for increase in surface area	$\tau_{\text{SA}}$				750
Time constant for increase in permeability	$\tau_{\text{perm}}$				$4 \times 10^4$
Albumin scaling factor	$A_{\text{albumin}}$				$4 \times 10^4$

### Glomerular hypertrophy

The glomerular ultrafiltration coefficient  $K_f$  represents both the permeability and the surface area of the glomerular membrane. When  $K_f$  was allowed to increase over time in response to changes in glomerular pressure (up to limit of 50%, the maximum increase observed in diabetic and/or nephrectomized rats, mice, and humans<sup>13,21,22</sup>), to represent increased glomerular filtration surface area with hypertrophy, glomerular pressure increased less while  $GFR$  increased further, suggesting that hypertrophy is an adaptive response that limits diabetes-induced increases in glomerular pressure (Fig. 3–light blue). The time constant  $\tau_{\text{SA}}$ , which determines the speed at which glomerular hypertrophy occurs, was set such that glomerular hypertrophy occurred quickly and would reach equilibrium within 3 months.

There is a large degree of variability in glucose levels among studies in db/db mice. The shaded regions in Fig. 3 show the predicted ranges for each variable as steady-state glucose varied from a lower bound of 250 to an upper bound of 600 mg/dl.

Figure 5 (blue lines) shows the effects of allowing glomerular pressure to drive a decrease in  $K_f$  due to glomerulosclerosis, a decrease in the number of nephrons, and an increase in the glomerular protein sieving rate over time. Parameters governing these relationships, as given in Table 1, were chosen in order to best fit the experimental data. Figures S1–S3 in the Supplemental Material show the sensitivity of the simulation results to varying values for these time constants.

$K_f$  increased during the first few weeks due to hypertrophy, but eventually began to decrease as hypertrophy reached its maximum and effects of glomerular pressure on glomerulosclerosis accumulated. The number of nephrons also began to decline over time, as glomerular pressure began to increase. As  $K_f$  and nephron number decreased,  $GFR$  began to decrease, although it remained above normal levels. While  $GFR$  decreased, the glomerular pressure required to achieve this  $GFR$  increased further.

### Modeling hyperfiltration and proteinuria in the db/db UNX mouse model

Progression of kidney disease and development of overt proteinuria in db/db mice are accelerated by uninephrectomy. We next tested whether our mathematical model could reproduce and explain changes in  $GFR$  and proteinuria that occur in db/db UNX mice, using parameters for disease progression determined above for db/db mice. To simulate db/db with UNX, we simulated diabetes as before, and then reduced the number of nephrons by half after 8 weeks of simulation time (UNX in the studies included in Fig. 2 were all conducted between weeks 8 and 10).

As shown in Fig. 5, following uninephrectomy at week 8,  $GFR$  was acutely reduced, but increased towards prior levels (and above non-diabetic levels) over the next few weeks, consistent with experimental observations. Because the increase in  $K_f$  due to hypertrophic surface area increase was already near its upper limit



**Table 2.** Observed (literature) and simulated phenotypic behavior in each species

Output parameters			Human		Rat		Mouse		References 15–23, 42–50
	Units	Symbols	Sim.	Lit.	Sim.	Lit.	Sim.	Lit.	
Glomerular Filtration Rate	ml/min	<i>GFR</i>	105	105 ± 15	2.5	1.9 ± 0.7	0.3	0.35 ± 0.1	
Single Nephron GFR	nl/min	<i>SNGFR</i>	55	52 ± 8	50	50 ± 10	29	33 ± 5	
Sodium Excretion	mEq/day	<i>Na<sub>ex</sub></i>	100	100 ± 15	2	2 ± 0.6	0.576	0.58 ± 0.02	
Mean Arterial Pressure	mmHg	<i>MAP</i>	93	90 ± 20	103	98 ± 5	98	98 ± 5	
Glomerular Pressure	mmHg	<i>P<sub>gc</sub></i>	60	60 ± 15	42	38 ± 5	37.5	38 ± 5	
Cardiac Output	l/min	<i>CO</i>	5	5 ± 0.7	0.4	0.4 ± 0.2	0.088	0.08 ± 0.04	
Renal Blood Flow	ml/Min	<i>RBF</i>	1100	10 <sup>3</sup> ± 300	11	10 ± 3	1.8	1.6 ± 0.25	

following induction of diabetes (glomerular volume increases by at most 50% in diabetes<sup>13,21</sup>), *GFR* could not increase further. At the same time, elevated glomerular pressure began driving glomerulosclerosis—a slower process of matrix deposition that thickens the glomerular basement membrane and reduces glomerular permeability. In addition, elevated glomerular pressure drove additional nephron loss over time. As  $K_f$  and nephron number decreased, glomerular pressure increased even further to maintain the *GFR* necessary for  $\text{Na}^+$  balance. The increase in glomerular pressure increased protein sieving and UAER. The magnitude and time course of UAER changes were consistent with the experimentally observed, higher level of and progressively increasing proteinuria in uninephrectomized mice.

## DISCUSSION

In this study, we adapted a mathematical model of renal physiology and function from human to mice, and incorporated adaptive and pathological mechanisms of diabetes and nephrectomy to describe changes in *GFR* and proteinuria observed in experimental db/db and db/db UNX mouse models. By changing a small number of parameters describing renal morphology, water and  $\text{Na}^+$  intake, as well as plasma protein concentration, the model reproduced differences and similarities in normal renal function between species. Nephron structure is conserved across species, in terms of morphology, as well as arteriole and tubule diameters<sup>25</sup>; significant cross-species differences are numbers of nephrons, which vary by orders of magnitude, and smaller differences in tubule segment lengths. Thus, while total *GFR*, *RBF*, and *RVR* may vary by order(s) of magnitude between species, at the single-nephron level, pressures and flow rates (and associated mechanical stretch and shear stress) experienced by cells within the glomeruli and tubules, as well as single-nephron filtered loads of reabsorbed substances such as  $\text{Na}^+$  and glucose, appear to be similar across mouse, rat, and human mammalian species. This suggests there is an optimal mechanical and biochemical environment for glomerular and tubular cells and tissues. Indeed, nephron morphogenesis has been shown to be directed in part by fluid flow.<sup>26</sup> Thus, it is to be expected that alterations which impact pressure and flow rate would lead to adaptations. Glomerular volume has been found to vary inversely with nephron number, which suggests hypertrophy is a compensatory response to allow for *GFR* to be maintained.<sup>27,28</sup> Based on this, we considered, in this analysis, the role of glomerular hypertrophy as a response to elevated glomerular capillary pressure.

We previously demonstrated, mathematically [12], the tubular hypothesis of diabetic hyperfiltration:<sup>10,29</sup> increased filtration is a necessary consequence of increased PT  $\text{Na}^+$  reabsorption in diabetes, and is required to restore  $\text{Na}^+$  balance. It is achieved through a combination of TGF, changes in Bowman's pressure, and  $\text{Na}^+$  retention, leading to increased net filtration pressure and

glomerular hypertension. A key physiological principle incorporated in the model is the requirement for  $\text{Na}^+$  balance. When PT  $\text{Na}^+$  reabsorption is increased, a  $\text{Na}^+$  imbalance is generated, which is compensated for by a combination of increased filtration and decreased reabsorption through other mechanisms [12]. In this paper, we extended the model to directly account for reabsorption of filtered glucose and  $\text{Na}^+$  through SGLT2, and we showed that by changing only blood glucose and  $\text{Na}^+$  intake from normal to db/db levels, the model reproduced the glomerular hyperfiltration observed in db/db mice. Hyperfiltration was initially achieved through elevations in mean arterial pressure and glomerular capillary hydrostatic pressure. Simulations demonstrated that increases in preglomerular arteriole diameters observed in diabetes prevent an excessive rise in mean arterial pressure, yet allow systemic blood pressure to be transmitted more directly to the glomerulus. Glomerular hypertrophy (represented as an increase in  $K_f$  due to increased glomerular surface area) in response to elevated glomerular pressure served to mitigate glomerular pressure increases, while maintaining the same *GFR*.

Similarly, uninephrectomy, represented in the model by reducing the number of nephron by half, initially produced a  $\text{Na}^+$  imbalance, which was quickly restored by both hyperfiltration of remaining nephrons (increased *SNGFR*, driven by a further increase in glomerular pressure) and decreased distal reabsorption, so that *GFR* returned to near normal. Elevated glomerular pressure is assumed to drive hypertrophy, but hypertrophic growth is not unlimited. Following diabetes initiation, simulations suggest that hypertrophic growth is already near maximum. After nephrectomy, as  $\text{Na}^+$  is retained and glomerular pressure begins to increase,  $K_f$  cannot increase further to compensate. Thus, glomerular pressure rises and remains elevated. Elevated glomerular pressure then rapidly begins to damage podocytes, allowing protein filtration and producing overt proteinuria, as is observed in db/db UNX mice. The model also predicts small rises in mean arterial pressure in the db/db mice, and much larger increases in db/db UNX mice. Experimentally, blood pressure is not often measured in these animals, but studies which did measure it report highly variable levels of increases, with changes in blood pressure ranging from negligible to as much as 40 mmHg.<sup>30,31</sup>

Our model-based simulations illustrate a general concept that is not specific to diabetic hyperfiltration: to maintain homeostasis, there is a level of *GFR* that needs to be achieved to maintain  $\text{Na}^+$  excretion sufficient for  $\text{Na}^+$  balance. *GFR* is proportional to  $K_f$  and net filtration pressure. Thus, as  $K_f$  increases, the necessary *GFR* (and thus  $\text{Na}^+$  balance) can be achieved with a lower glomerular hydrostatic pressure. This supports a role for glomerular hypertrophy as an adaptive response, to prevent exposure of glomeruli to deleterious elevations in glomerular pressure.

Glomerular hypertension is associated with progressive deposition of excess glomerular extracellular matrix and formation of glomerular lesions, and therapies such as ACE inhibitors, which

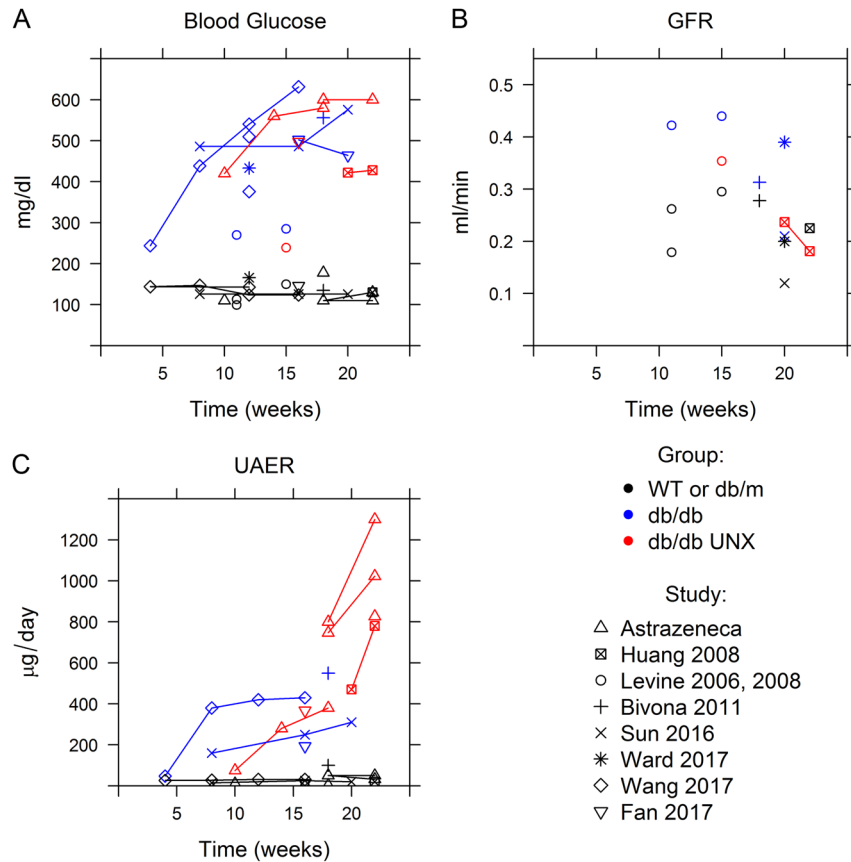


**Fig. 2** Blood glucose, *GFR*, and UAER over time in db/db mice with or without uninephrectomy (UNX—performed between 8–10 weeks of age), compared to WT or db/m mice. Data were obtained from published studies (Huang 2008,<sup>12</sup> Levine 2006,<sup>46</sup> Levine 2008,<sup>13</sup> Bivona 2011,<sup>21</sup> Sun 2016,<sup>47</sup> Ward 2017,<sup>48</sup> Wang 2017,<sup>49</sup> and Fan 2017<sup>50</sup>) and unpublished AstraZeneca reports of additional studies conducted according to protocols of Huang 2008<sup>12</sup>

reduce glomerular hydrostatic pressure, have been shown to slow this process.<sup>32,33</sup> In db/db mice, this occurs rather slowly, with substantial glomerular basement membrane (GBM) thickening occurring over 6–12 months.<sup>7</sup> In db/db UNX mice, it occurs much faster, with significant GBM thickening by 22 weeks. In our model, glomerular hypertension causes slow but cumulative and irreversible reductions in membrane permeability over time. We recognize that other factors, including inflammation and release of growth factors by mesangial cells and podocytes, may contribute as well. However these factors were not considered in the current model. In the simulated db/db mice, the hypertrophic response dominated, and the net increase in  $K_f$  allowed glomerular pressure to be normalized, with very little loss of membrane permeability. However, in the simulated db/db UNX model, once the hypertrophic increase in surface area reached its limit,  $K_f$  began to decrease. As  $K_f$  decreased, glomerular hydrostatic pressure had to increase further in order to maintain *GFR* and  $\text{Na}^+$  balance. The further increase in glomerular pressure led to more proteinuria and further GBM thickening. Thus, the model provides an elegant mechanistic explanation for hyperfiltration, progression of proteinuria and GBM thickening observed in db/db UNX mice.

This analysis focuses on hemodynamic mechanisms of kidney injury in diabetes. Diabetes being an overly complex disease process, many other factors, including inflammatory, neurohumoral, and genetic ones are likely important.<sup>34</sup> The model also used a simplified representation of renal structure and function; additional complexities such as normal variability in nephron number or differences in architectural organization across species were not considered. Also, we did not attempt to model the contribution of various transporters in detail. This has been done

quite elegantly by others,<sup>35–37</sup> and we believe that the current representation was sufficient to explore the questions addressed in this study.

In conclusion, we adapted a mathematical model of renal function from human to mice, and incorporated adaptive and pathological mechanisms of diabetes and nephrectomy to describe changes in *GFR* and proteinuria observed in the experimental db/db and db/db uninephrectomy (UNX) mice. The model was able to reproduce experimentally observed trends, and thus provides a mechanistic explanation for the hyperfiltration and proteinuria responses observed in db/db and db/db UNX mice. Such a quantitative, mechanistically-oriented disease model may well serve as a platform for quantitatively exploring pharmacological mechanisms in a preclinical setting and for evaluating translational aspects of experimental drug effects from the db/db UNX model to specific diabetes and renal disease patient populations.

## METHODS

The base model of renal function is summarized in Fig. 3, and described in detail in ref. <sup>38</sup> Full model equations are included in the Supplemental Material. Briefly, this model describes key physiological processes involved in renal function and their roles in maintaining  $\text{Na}^+$  and water homeostasis. It describes blood flow, resistance, and pressures through the renal vasculature; filtration of water and  $\text{Na}^+$  through the glomerulus;  $\text{Na}^+$  and water reabsorption, flow rates, and pressures in each tubular segment;  $\text{Na}^+$  and water excretion;  $\text{Na}^+$  and water balance and its effects on interstitial fluid volume and blood pressure. Key regulatory feedback mechanisms are incorporated in the model, including the renin-angiotensin-aldosterone system (RAAS), TGF, myogenic autoregulation,

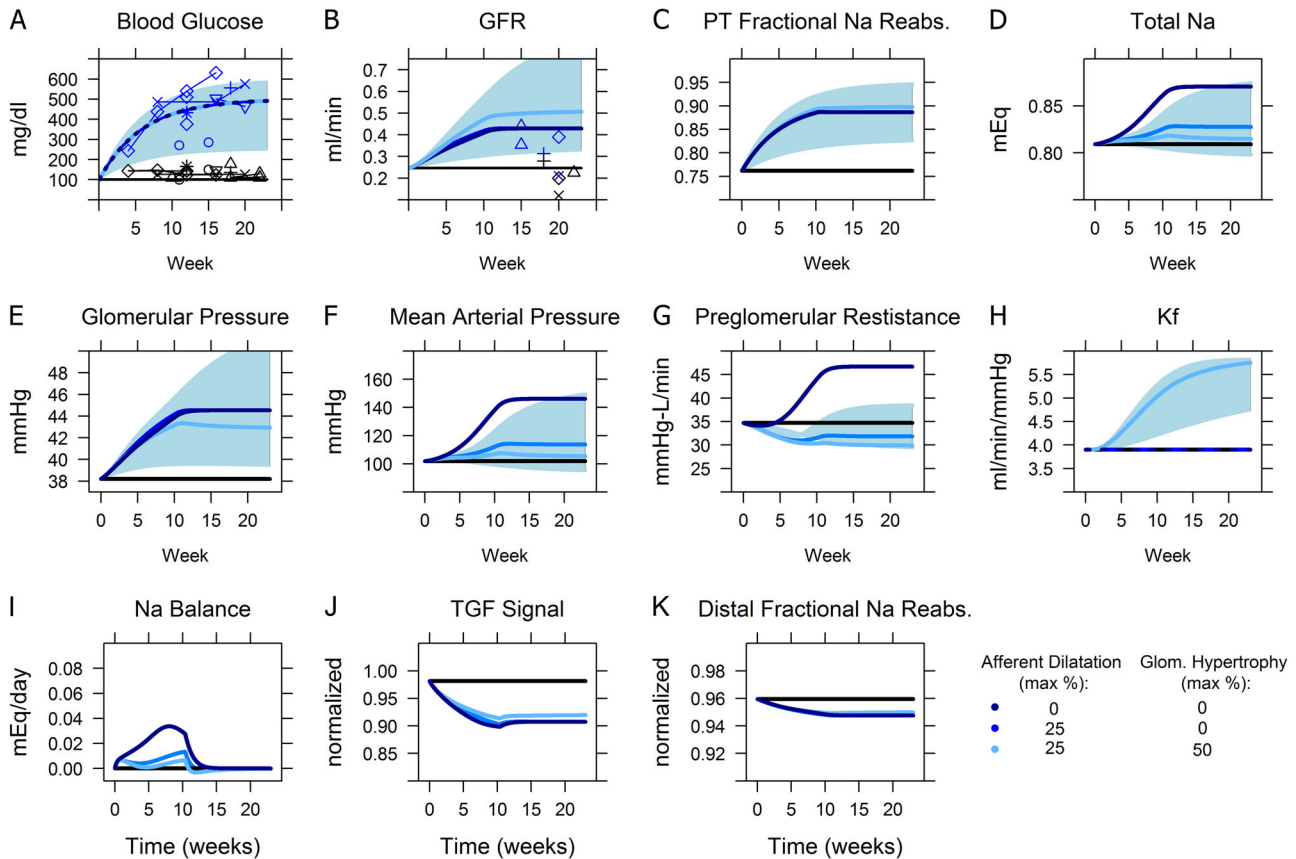


**Fig. 3** Simulated responses to development of diabetes (simulated as a progressive increase in blood glucose, sodium intake, and renal threshold for glucose excretion) in db/db mice, and the effect of afferent dilatation and glomerular hypertrophy. Solid lines: simulations (light, medium and dark blue solid lines: db/db mice, black line: simulated non-db mice) points: experimental data (blue: db/db mice, black: WT or db/m mice). See Fig. 2 for data references. Shaded area: range of response as blood glucose varied from 250 to 600 mg/dl, under conditions of 25% afferent dilatation and 50% glomerular hypertrophy. Increasing blood glucose **a** and the associated increase in PT sodium reabsorption **c** caused sodium retention **d** and increases in mean arterial pressure **f** and glomerular pressure **g**, until *GFR* increased sufficiently to return sodium balance **i** and prevent further sodium accumulation. Afferent dilatation prevented preglomerular resistance **g** from rising and allowed the necessary hyperfiltration to be achieved at lower MAP, while glomerular hypertrophy **h** allowed it to be achieved at lower glomerular pressure

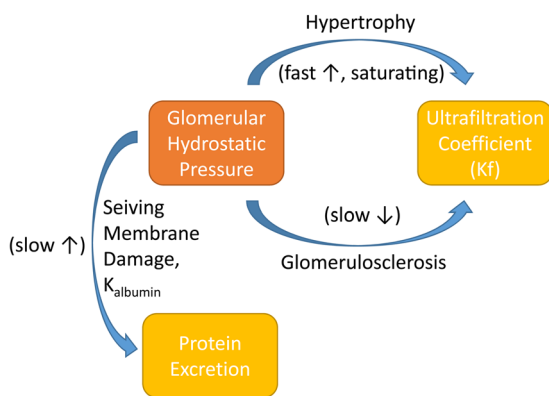


**Fig. 4** Modeling of adaptive and maladaptive (pathological) effects of elevated glomerular hydrostatic pressure. When glomerular pressure is increased above normal, glomeruli adapt by growing, thereby increasing the filtering surface area and the associated ultrafiltration coefficient  $K_f$  in a relatively fast (over the course of weeks) saturating process. At the same time, elevated glomerular pressure initiates glomerulosclerosis, a much slower and non-saturating process that increases the basement membrane thickness, thus reducing permeability and lowering  $K_f$ . Elevated glomerular pressure also damages the podocytes, effectively increasing the protein sieving coefficient

effects of renal interstitial hydrostatic pressure (RIHP) on regulation of tubular  $\text{Na}^+$  reabsorption, vasopressin regulation of tubular water reabsorption, and local blood flow autoregulation.

We here extended this model to: (1) account for glucose filtration, reabsorption through SGLT2, and excretion, (2) explicitly account for the coupling of  $\text{Na}^+$  with glucose reabsorption through SGLT2, (3) account for filtration, reabsorption, and excretion of albumin, and (4) simulate adaptive and maladaptive changes in the glomerulus, in response to increased glomerular pressure (afferent and glomerular hypertrophy, glomerulosclerosis, podocyte damage).

In this model (see Fig. 1), single nephron glomerular filtration rate (SNGFR) is defined according to Starling's equation, where  $K_f$  is the glomerular ultrafiltration coefficient,  $P_{gc}$  is glomerular capillary hydrostatic pressure,  $P_{Bow}$  is pressure in the Bowman's space, and  $\pi_{go-avg}$  is average glomerular capillary oncotic pressure:

$$SNGFR = K_f(P_{gc} - P_{Bow} - \pi_{go-avg}) \quad (1)$$

The total *GFR* is then the *SNGFR* multiplied by the number of nephrons:

$$GFR = SNGFR * N_{nephrons} \quad (2)$$

#### Glucose filtration and reabsorption

Glucose is filtered freely through the glomerulus, so that single nephron filtered glucose load is:

$$\phi_{glu,filtered} = SNGFR * C_{glu} \quad (3)$$

where  $C_{glu}$  is the plasma glucose concentration.

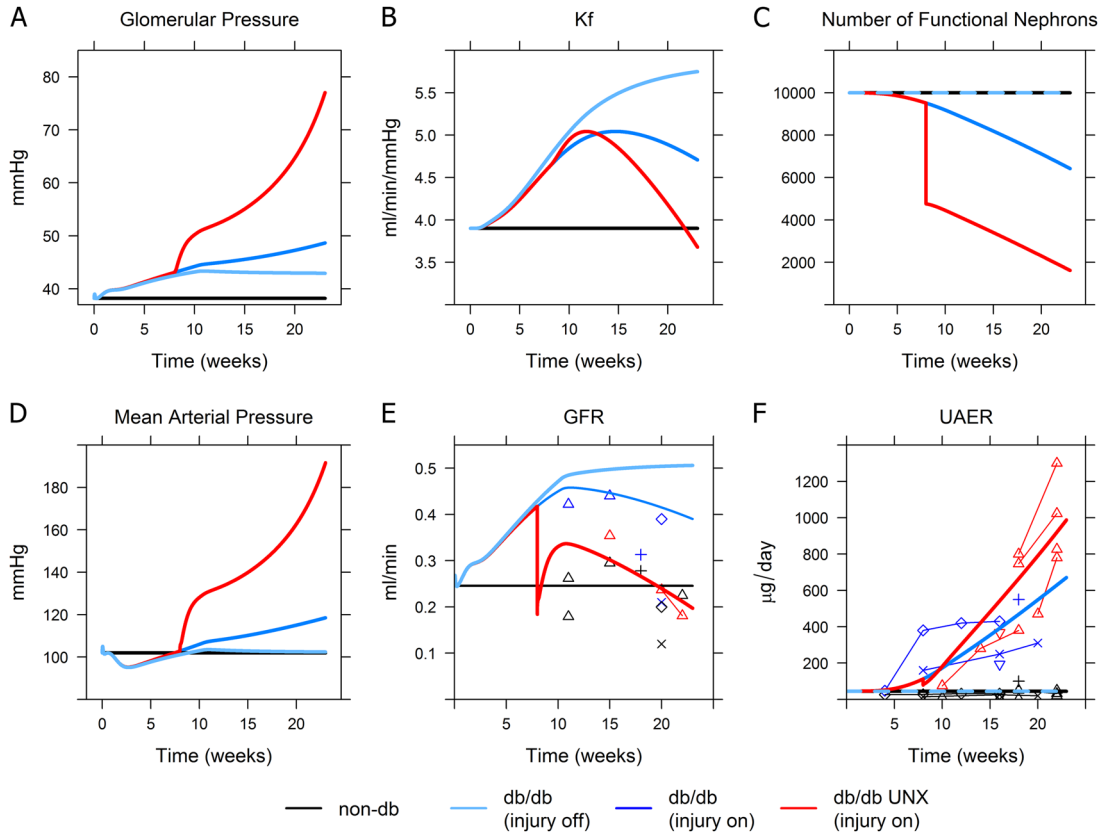


**Fig. 5** Simulated effects of pressure-induced nephron injury and uninephrectomy on disease progression in db/db mice. Solid lines: simulations (black: non-db, light blue – db/db non-UNX with injury effects turned off, dark blue–db/db non-UNX with injury effects turned on, red–db/db UNX with injury effects turned on). Points: experimental data (black non-db, blue – db/db, red – db/db UNX). See Fig. 2 for data references. In db/db non-UNX mice, when injury effects were turned on, elevated glomerular pressure (a) caused  $K_f$  to peak and then begin to decrease (b), as the effect of glomerular hypertrophy saturated while the effect of glomerulosclerosis grew; elevated glomerular pressure also drove a decrease in nephron number (c) and an increase in glomerular albumin sieving.  $GFR$  (e) increased over time but eventually began to decrease slowly around week 10, while glomerular pressure (a) and UAER (f) progressively increased, in agreement with experimental data. When UNX was simulated at 8 weeks,  $GFR$  initially dropped but recovered before beginning to progressively decline. This progression was driven by a further increase in glomerular pressure, and an accelerated rate of glomerulosclerosis ( $K_f$  decrease) and nephron loss

Glucose reabsorption occurs exclusively in the PT through  $\text{Na}^+$  glucose cotransporters (SGLT). SGLT2 in the S1 and S2 segments of the PT reabsorbs 90 to 97% of filtered glucose, while SGLT1 in the S3 segment reabsorbs the remaining 3 to 10%.<sup>10,39</sup> As long as the filtered glucose load remains below the reabsorptive capacity of SGLT in the PT, glucose is nearly completely reabsorbed, and excreted glucose is negligible. However, at high plasma concentrations, filtered glucose can exceed the kidney's capacity for reabsorption, and the excess glucose is excreted. The plasma concentration at which filtered glucose exceeds the renal capacity for glucose reabsorption has been defined as the renal threshold for glucose excretion,  $RT_G$ . The renal capacity for glucose reabsorption, or  $RC_{\text{glucose}}$ , is given by:

$$RC_{\text{glucose}} = RT_G * SNGFR \quad (4)$$

The rate of glucose reabsorption is then:

$$\phi_{\text{glu, reabs}} = \min(\phi_{\text{glu, filtered}}, RC_{\text{glucose}}) \quad (5)$$

Any non-reabsorbed glucose is then excreted, so that the rate of urinary glucose excretion ( $R_{\text{UGE}}$ ) is:

$$R_{\text{UGE}} = \phi_{\text{glu, filtered}} - \phi_{\text{glu, reabs}} \quad (6)$$

$\text{Na}^+$  filtration and reabsorption in the PT

Similarly to glucose,  $\text{Na}^+$  is freely filtered across the glomerulus, so that the single nephron-filtered  $\text{Na}^+$  load is given by:

$$\phi_{\text{Na, filtered}} = SNGFR * C_{\text{Na}} \quad (7)$$

where  $C_{\text{Na}}$  is the plasma  $\text{Na}^+$  concentration.

Assuming that glucose reabsorption through SGLT1 is small compared to reabsorption through SGLT2, the rate of  $\text{Na}^+$  reabsorption through SGLT2 is approximately equal to the rate of glucose reabsorption:

$$\phi_{\text{Na, reabs-SGLT2}} = \phi_{\text{glu, reabs}} \quad (8)$$

Total PT  $\text{Na}^+$  reabsorption is then given by:

$$\phi_{\text{Na, reabs-PT}} = \phi_{\text{Na, filtered}} * \eta_{\text{pt, non-SGLT2}} + \phi_{\text{Na, reabs-SGLT2}} \quad (9)$$

where  $\eta_{\text{pt, non-SGLT2}}$  is the fractional rate of PT reabsorption through mechanisms other than SGLT2.  $\text{Na}^+$  flow rate out of the PT is then:

$$\phi_{\text{Na, out-PT}} = \phi_{\text{Na, filtered}} - \phi_{\text{Na, reabs-PT}} \quad (10)$$

$\text{Na}^+$  reabsorption along the rest of the tubule is modeled as in ref.<sup>11</sup>

Albumin filtering and excretion

The rate of albumin filtration is a function of SNGFR, the plasma albumin concentration  $C_{\text{albumin}}$  and the sieving coefficient  $K_{\text{albumin}}$ , as described in<sup>40</sup>:

$$\phi_{\text{albumin, filtered}} = K_{\text{albumin}} * SNGFR * C_{\text{albumin}} \quad (11)$$

The proximal tubule has the capacity to reabsorb a limited amount of filtered albumin ( $RC_{\text{albumin}}$ ), beyond which excess albumin is excreted.

$$\phi_{\text{albumin, reabs}} = \min(\phi_{\text{albumin, filtered}} * \eta_{\text{albumin}}, RC_{\text{albumin}}) \quad (12)$$

The urinary albumin excretion rate (UAER) is then:

$$UAER = (\phi_{\text{albumin, filtered}} - \phi_{\text{albumin, reabs}}) * N_{\text{nephrons}} \quad (13)$$



## Kidney adaptation and injury in response to diabetes and glomerular hypertension

Afferent arteriole diameter is increased in db/db mice, although the precise underlying mechanism has not been established. Thus, we modeled the dilatation as a function of blood glucose, without prescribing intermediate mechanisms. The arteriole diameter  $D_{aa}$  was allowed to increase up to a maximum  $\Delta D_{aa}$  of 25%, and the rate of increase was proportional to the difference between blood glucose (BG) and nominal blood glucose of 90 mg/dl, with a time constant  $\tau_{daa}$ .

$$\frac{d}{dt}(\Delta D_{aa}) = (\Delta D_{aa\max} - \Delta D_{aa}) * \frac{\max(BG - BG_{\text{nom}}, 0)}{\tau_{daa}} \quad (19)$$

We assumed that, when glomerular capillary hydrostatic pressure  $P_{gc}$  rises above some normal limit  $P_{gc,0}$ , it begins to drive both adaptive and pathophysiological changes in the glomerulus. The magnitude of this damage signal is defined as:

$$\text{GP\_damage\_effect} = \max\left(\frac{P_{gc}}{P_{gc,0}} - 1, 0\right) \quad (14)$$

The ultra-filtration coefficient  $K_f$ , in Eq. 1 above, reflects both the permeability and surface area of the glomerular membrane. The effect of glomerular pressure on  $K_f$  through changes in the glomerular surface area (hypertrophy) is modeled as:

$$\frac{d}{dt}(\Delta SA) = (\Delta SA_{\max} - \Delta SA) * \frac{\text{GP\_damage\_effect}}{\tau_{SA}} \quad (15)$$

$\Delta SA_{\max}$  is the maximum increase in glomerular surface area (SA; expressed as a percentage).  $\tau_{SA}$  represents the time constant for the increase in surface area.  $\Delta SA_{\max}$  is fixed at 50%, the maximum increase observed in diabetic and/or nephrectomized rats, mice, and humans.<sup>13,21,22</sup> The time constant  $\tau_{SA}$  is set so that a steady-state is reached within a few weeks.

The effect of glomerular pressure on  $K_f$ , through reductions in the glomerular permeability (glomerulosclerosis), is modeled as:

$$\frac{d}{dt}(\Delta Perm) = (\Delta Perm_{\max} - \Delta Perm) * \frac{\text{GP\_damage\_effect}}{\tau_{perm}} \quad (16)$$

$\Delta Perm_{\max}$  is the maximal decrease in permeability (in percentage).  $\tau_{perm}$  represents the time constant for the decrease in permeability.  $\Delta Perm_{\max}$  is assumed to be 100%, so that, eventually, permeability can decrease to zero.

The ultrafiltration coefficient  $K_f$  is then given by:

$$K_f = K_{f,0} * (1 + \Delta SA - \Delta Perm) \quad (17)$$

where  $K_{f,0}$  is the normal ultrafiltration coefficient in the healthy state.

The effect of glomerular pressure on nephron loss is modeled as:

$$\frac{d}{dt}(\Delta \text{Nephrons}) = (1 - \Delta \text{Nephrons}) * \frac{\text{GP\_damage\_effect}}{\tau_{\text{nephronLoss}}} \quad (17)$$

$\Delta \text{Nephrons}$  is the percentage of total nephrons lost,  $\tau_{\text{nephronLoss}}$  represents the time constant for nephron loss.

Glomerular hypertension also damages to podocytes, causing them to leak protein. This is modeled as an increase in the sieving coefficient, in response to increased glomerular pressure:

$$\frac{d}{dt}(\Delta K_{\text{albumin}}) = \frac{\text{GP\_damage\_effect}}{\tau_{\text{nephronLoss}}} \quad (18)$$

$$K_{\text{albumin}} = K_{\text{albumin},0} + \Delta K_{\text{albumin}} \quad (19)$$

$K_{\text{albumin},0}$  is the sieving coefficient under normal conditions, and  $\tau_{\text{albumin}}$  is a time constant for the effect of glomerular pressure on sieving damage. Changes in albumin excretion in response to glomerular hypertension occur quickly, and thus this time constant is much larger than the other time constants (see Table 2). This is consistent with the fast changes in proteinuria observed with antihypertensive treatments, and in diseases such as preeclampsia.

## Model software and implementation

The model was implemented in the open-source programming software R 3.1.2, using the *RxODE* package<sup>41</sup>.

## DATA AVAILABILITY

The authors declare that [the/all other] data supporting the findings of this study are available within the paper [and its supplementary information files], or in previous publications as referenced within the paper.

## ACKNOWLEDGEMENTS

The project is funded by AstraZeneca Pharmaceuticals.

## AUTHOR CONTRIBUTIONS

K.M.H., C.A., R.J.L., and G.H., P.G. were involved in study design and development. H.S.M., K.M.H., and U.J. analyzed data. K.M.H., H.S.M., C.A., R.J.L., and G.H. interpreted data. K.M.H. and H.S.M. drafted manuscript. K.M.H., H.S.M., C.A., R.J.L., U.J., and G.H. edited and revised manuscript.

## ADDITIONAL INFORMATION

**Supplementary information:** accompanies the paper on the *npj Systems Biology and Applications* website (<https://doi.org/10.1038/s41540-018-0077-9>).

**Competing interests:** C.A., R.J.L., U.J., and G.H. are employees of AstraZeneca Pharmaceuticals. M.H. and H.S.M. have received research funding from AstraZeneca Pharmaceuticals.

**Publisher's note:** Springer Nature remains neutral with regard to jurisdictional claims in published maps and institutional affiliations.

## REFERENCES

- Montero, R. M., C. A., Gnudi, L. & Goldsmith, D. Diabetic nephropathy: What does the future hold? *Int. Urol. Nephrol.* **48**, 99–113 (2016).
- van Hasselt, J. G. & van der Graaf, P. Towards integrative systems pharmacology models in oncology drug development. *Drug Discov Today Technol.* **15**, 1–8, <https://doi.org/10.1016/j.ddtec.2015.06.004> (2015).
- Bohle, A. et al. The Pathogenesis of Chronic-Renal-Failure in Diabetic Nephropathy - Investigation of 488 Cases of Diabetic Glomerulosclerosis. *Pathol. Res. Pract.* **187**, 251–259 (1991).
- Cherney, A. N. Sa. D. Z. Renal hyperfiltration related to diabetes mellitus and obesity in human disease. *World J. Diabetes* **3**, 1–6 (2012).
- Hudkins, K. L. et al. BTBR Ob/Ob Mutant Mice Model Progressive Diabetic Nephropathy. *J. Am. Soc. Nephrol.* **21**, 1533–1542 (2010).
- Pichaiwong, W. et al. Reversibility of Structural and Functional Damage in a Model of Advanced Diabetic Nephropathy. *J. Am. Soc. Nephrol.* **24**, 1088–1102 (2013).
- Sharma, K., McCue, P. & Sr, D. Diabetic kidney disease in the db/db mouse. *Am. J. Physiol.-Ren. Physiol.* **284**, F1138–F1144 (2003).
- Koya, D. et al. Amelioration of accelerated diabetic mesangial expansion by treatment with a PKC beta inhibitor in diabetic db/db mice, a rodent model for type 2 diabetes. *FASEB J.* **14**, 439–447 (2000).
- Hallow, K. M. & Gebremichael, Y. A quantitative systems physiology model of renal function and blood pressure regulation: Model description. *CPT Pharmacomet. Syst. Pharmacol.* **6**, 383–392 (2017).
- Vallon, V. The proximal tubule in the pathophysiology of the diabetic kidney. *Am. J. Physiol.-Reg. Integr. Comp. Physiol.* **300**, R1009–R1022 (2011).
- Hallow, K. M., Helmlinger, G. Y. & Vallon, G. et al. Primary proximal tubule hyperreabsorption and impaired tubular transport counterregulation determine glomerular hyperfiltration in diabetes: a modeling analysis. *Am. J. Physiol.-Renal Physiol.* **312**(5), F819–F835 (2017).
- Huang, Y. et al. A PAI-1 mutant, PAI-1R, slows progression of diabetic nephropathy. *J. Am. Soc. Nephrol.* **19**, 329–338 (2008).
- Levine, D. Z., Iacovitti, M. & Robertson, S. J. Modulation of single-nephron GFR in the db/db mouse model of type 2 diabetes mellitus. II. Effects of renal mass reduction. *Am. J. Physiol.-Reg. Integr. Comp. Physiol.* **294**, R1840–R1846 (2008).
- Liang, Y. et al. Effect of Canagliflozin on Renal Threshold for Glucose, Glycemia, and Body Weight in Normal and Diabetic Animal Models. *PLoS One* **7**, e30555 (2012).
- Chodavarapu, H. et al. Rosiglitazone Treatment of Type 2 Diabetic db/db Mice Attenuates Urinary Albumin and Angiotensin Converting Enzyme 2 Excretion. *PLoS One* **8**, e62833 (2013).
- Park, S., Bivona, B. J., Feng, Y., Lazartigues, E. & Harrison-Bernard, L. M. Intact renal afferent arteriolar autoregulatory responsiveness in db/db mice. *Am. J. Physiol.-Ren. Physiol.* **295**, F1504–F1511 (2008).

17. Carmines, P. K. The renal vascular response to diabetes. *Curr. Opin. Nephrol. Hypertens.* **19**, 85–90 (2010).
18. Helal, I., Fick-Brosnahan, G. M., Reed-Gitomer, B. & Schrier, R. W. Glomerular hyperfiltration: definitions, mechanisms and clinical implications. *Nat. Rev. Nephrol.* **8**, 293–300 (2012).
19. Brenner, B. M. Nephron Adaptation to Renal Injury or Ablation. *Am. J. Physiol.* **249**, F324–F337 (1985).
20. Chen, K. W. et al. Compensatory Hypertrophy After Living Donor Nephrectomy. *Transplant. Proc.* **48**, 716–719 (2016).
21. Bivona, B. J., Park, S. & Harrison-Bernard, L. M. Glomerular filtration rate determinations in conscious type II diabetic mice. *Am. J. Physiol.-Ren. Physiol.* **300**, F618–F625 (2011).
22. Flyvbjerg, A. et al. Amelioration of long-term renal changes in obese type 2 diabetic mice by a neutralizing vascular endothelial growth factor antibody. *Diabetes* **51**, 3090–3094 (2002).
23. Abbate, M., Zoja, C. & Remuzzi, G. How does proteinuria cause progressive renal damage? *J. Am. Soc. Nephrol.* **17**, 2974–2984 (2006).
24. Li, B. et al. Real-time observation of glomerular hemodynamic changes in diabetic rats: effects of insulin and ARB. *Kidney Int.* **66**, 1939–1948 (2004).
25. Romagnani, P., Lasagni, L. & Remuzzi, G. Renal progenitors: an evolutionary conserved strategy for kidney regeneration. *Nat. Rev. Nephrol.* **9**, 137–146 (2013).
26. Vasilyev, A. et al. Collective cell migration drives morphogenesis of the kidney nephron. *PLoS Biol.* **7**, e9 (2009).
27. Luyckx, V. A., Shukha, K. & Brenner, B. M. Low nephron number and its clinical consequences. *Rambam Maimonides Med. J.* **2**, e0061 (2011).
28. Hoy, W. E. et al. Nephron number, glomerular volume, renal disease and hypertension. *Curr. Opin. Nephrol. Hypertens.* **17**, 258–265 (2008).
29. Vallon, V. & Thomson, S. C. Renal function in diabetic disease models: the tubular system in the pathophysiology of the diabetic kidney. *Annu. Rev. Physiol.* **74**, 351–375 (2012).
30. Senador, D., Kanakamedala, K., Irgoyen, M. C., Morris, M. & Elased, K. M. Cardiovascular and autonomic phenotype of db/db diabetic mice. *Exp. Physiol.* **94**, 648–658 (2009).
31. Bagi, Z. et al. Type 2 diabetic mice have increased arteriolar tone and blood pressure: enhanced release of COX-2-derived constrictor prostaglandins. *Arterioscler. Thromb. Vasc. Biol.* **25**, 1610–1616 (2005).
32. Anderson, S. & Brenner, B. M. The role of intraglomerular pressure in the initiation and progression of renal disease. *J. Hypertens. Suppl.* **4**, S236–S238 (1986).
33. Simons, J. L. et al. Modulation of glomerular hypertension defines susceptibility to progressive glomerular injury. *Kidney Int.* **46**, 396–404 (1994).
34. Thomas, M. C. et al. Diabetic kidney disease. *Nat. Rev. Dis. Prim.* **1**, 15018 (2015).
35. Weinstein, A. M. A mathematical model of the rat nephron: glucose transport. *Am. J. Physiol.-Ren. Physiol.* **308**, F1098–F1118 (2015).
36. Moss, R. & Layton, A. T. Dominant factors that govern pressure natriuresis in diuresis and antidiuresis: a mathematical model. *Am. J. Physiol.-Ren. Physiol.* **306**, F952–F969 (2014).
37. Layton, A. T., Vallon, V. & Edwards, A. Predicted Consequences of Diabetes and SGLT Inhibition on Transport and Oxygen Consumption along a Rat Nephron. *Am. J. Physiol.-Ren. Physiol.* **310**, F1269–F1283 (2016).
38. Gebremichael, Y. et al. Quantitative Systems Pharmacology Modeling of Drug-Induced Proximal Tubular (Pt) Injury. *Clin. Pharmacol. Ther.* **101**, S64–S64 (2017).
39. Vallon, V. et al. SGLT2 Mediates Glucose Reabsorption in the Early Proximal Tubule. *J. Am. Soc. Nephrol.* **22**, 104–112 (2011).
40. Lazzara, M. J. & Deen, W. M. Model of albumin reabsorption in the proximal tubule. *Am. J. Physiol.-Ren. Physiol.* **292**, F430–F439 (2007).
41. Wang, W., Hallow, K. M. & James, D. A. A Tutorial on RxODE: Simulating Differential Equation Pharmacometric Models in R. *CPT Pharmacomet. Syst. Pharmacol.* **5**, 3–10 (2016).
42. Bilan, V. P. et al. Diabetic nephropathy and long-term treatment effects of rosiglitazone and enalapril in obese ZSF1 rats. *J. Endocrinol.* **210**, 293–308 (2011).
43. Valk, E. J., Bruijn, J. A. & Bajema, I. M. Diabetic nephropathy in humans: pathologic diversity. *Curr. Opin. Nephrol. Hypertens.* **20**, 285–289 (2011).
44. Cowley, A. W. Jr. et al. Progression of glomerular filtration rate reduction determined in conscious Dahl salt-sensitive hypertensive rats. *Hypertension* **62**, 85–90 (2013).
45. Soler, M. J., Riera, M. & Batlle, D. New experimental models of diabetic nephropathy in mice models of type 2 diabetes: efforts to replicate human nephropathy. *Exp. Diabetes Res.* **2012**, 616313 (2012).
46. Levine, D. Z., Iacovitti, M., Robertson, S. J. & Mokhtar, G. A. Modulation of single-nephron GFR in the db/db mouse model of type 2 diabetes mellitus. *Am. J. Physiol.-Reg. Integr. Comp. Physiol.* **290**, R975–R981 (2006).
47. Sun, H. et al. Astragaloside IV ameliorates renal injury in db/db mice. *Sci. Rep.* **6**, 32545 (2016).
48. Ward, M. S. et al. Targeted mitochondrial therapy using MitoQ shows equivalent renoprotection to angiotensin converting enzyme inhibition but no combined synergy in diabetes. *Sci. Rep.* **7**, 15190 (2017).
49. Wang, X. X. et al. SGLT2 Protein Expression Is Increased in Human Diabetic Nephropathy: SGLT2 Protein inhibition decreases renal lipid accumulation, inflammation, and the development of nephropathy in diabetic mice. *J. Biol. Chem.* **292**, 5335–5348 (2017).
50. Fan, Y. et al. Rtn1a-Mediated Endoplasmic Reticulum Stress in Podocyte Injury and Diabetic Nephropathy. *Sci. Rep.* **7**, 323 (2017).



**Open Access** This article is licensed under a Creative Commons Attribution 4.0 International License, which permits use, sharing, adaptation, distribution and reproduction in any medium or format, as long as you give appropriate credit to the original author(s) and the source, provide a link to the Creative Commons license, and indicate if changes were made. The images or other third party material in this article are included in the article's Creative Commons license, unless indicated otherwise in a credit line to the material. If material is not included in the article's Creative Commons license and your intended use is not permitted by statutory regulation or exceeds the permitted use, you will need to obtain permission directly from the copyright holder. To view a copy of this license, visit <http://creativecommons.org/licenses/by/4.0/>.

© The Author(s) 2018